Ocean acidification in emission-driven temperature stabilization scenarios: the role of TCRE and non-CO_2 greenhouse gases

Jens Terhaar[1,2,3], Thomas L. Frölicher[1,2], Fortunat Joos[1,2]

[1] Climate and Environmental Physics, Physics Institute, University of Bern, Switzerland

[2] Oeschger Centre for Climate Change Research, University of Bern, Switzerland

[3] Department of Marine Chemistry and Geochemistry, Woods Hole Oceanographic Institution, 360 Woods Hole Road, Woods Hole, 02543, Massachusetts, USA

E-mail: jens.terhaar@unibe.ch

Abstract

Future ocean acidification mainly depends on the continuous ocean uptake of CO_2 from the atmosphere. The trajectory of future atmospheric CO_2 is prescribed in traditional climate projections with Earth System Models, leading to a small model spread and apparently low uncertainties for projected acidification, but a large spread in global warming. However, climate policies such as the Paris Agreement define climate targets in terms of global warming levels and as traditional simulations do not converge to a given warming level, they cannot be used to assess uncertainties in projected acidification. Here, we perform climate simulations that converge to given temperature levels using the Adaptive Emission Reduction Algorithm (AERA) with the Earth System Model Bern3D-LPX at different setups with different transient climate response to cumulative carbon emissions (TCRE) and choices between reductions in CO_2 and non-CO_2 forcing agents. With these simulations, we demonstrate that uncertainties in surface ocean acidification are an order of magnitude larger than the usually reported inter-model uncertainties from simulations with prescribed atmospheric CO_2. Uncertainties in acidification at a given stabilized temperature are dominated by TCRE and the choice of emission reductions of non-CO_2 greenhouse gases. High TCRE and relatively low reductions of non-CO_2 greenhouse gases, for example, necessitate relatively strong reductions in CO_2 emissions and lead to relatively little ocean acidification at a given temperature level. The results suggest that choices between reducing emissions of CO_2 versus non-CO_2 agents should consider the economic costs and ecosystem damage of ocean acidification.

Keywords: Ocean acidification, Paris agreement, uncertainties

1. Introduction

The Paris Agreement aims at limiting global warming well below 2°C and at pursuing efforts to reduce warming to 1.5°C to significantly reduce the risks and impacts of climate change [1]. To stabilize temperatures, the sum of CO_2 forcing equivalent (CO_2-fe) emissions [2,3] from all greenhouse gases (GHGs) together must be close to net-zero [4–7]. The remaining allowable emissions of CO_2 and non-CO_2 forcing agents that can be emitted before net-zero must be reached depends among others on the transient climate response to cumulative emissions (TCRE), i.e., the amount of warming per amount of cumulative emissions. TCRE depends on the transient climate response (or equilibrium climate sensitivity) and the strength of the ocean and land carbon sinks [2,5,8–16]. These allowable emissions can be distributed over all GHGs in many combinations. If relatively strong reductions in non-CO_2 greenhouse gas emissions would be implemented, for example, the remaining allowable CO_2 emissions will be relatively higher.

Globally averaged atmospheric surface warming is the main and often only measure of success or failure of the Paris Agreement, although climate impacts and stressors of ecosystems do not only or sometimes not at all depend on the level of global warming [17–19]. One example of such a potential ecosystem stressor is ocean acidification, a process that describes the gradual decrease in ocean pH, carbonate ions, and calcium carbonate mineral saturation states (Ω) in the ocean, which affects a variety of individual calcifying marine organisms and has the potential to disrupt entire ecosystems [20–30].

Future ocean acidification depends mainly on CO_2 emissions and the perturbation in atmospheric and oceanic carbon cycle and is only marginally affected by the degree of warming [31], except in the Arctic Ocean [31,32]. In surface waters, equilibrating rapidly with the atmosphere, acidification is primarily driven by atmospheric CO_2 [23,24,33], with a regional role for alkalinity changes, e.g. in estuaries and the Arctic Ocean [34–38]. Acidification at depth depends mainly on how much of the anthropogenic carbon perturbation at the surface is transported to the deeper ocean [39–43].

As trajectories of future atmospheric CO_2 are prescribed in the simulations from the Coupled Model Intercomparison Project (CMIP) by the socio-economic pathways [44,45] that are used by the regular IPCC reports [46,47], projections of ocean acidification have usually very low to non-existent model uncertainties at the ocean surface [18,19,33,37,48]. Therefore, these simulations cannot directly be used to inform policy makers about the uncertainties in ocean acidification and might, in the

worst case, lead to overly confident projections on ocean acidification used for impact assessments. Only few studies assess uncertainties in projected ocean acidification comprehensively with prescribed carbon emissions by using perturbed parameter ensembles in simulations or by quantifying uncertainties as a function of cumulative carbon emissions [17,49,50]. These studies quantify uncertainties related to the land and ocean carbon sink but neither quantify uncertainties from the choice of greenhouse gas reductions (CO_2 vs non-CO_2) nor from the transient climate response to emissions. Such studies that quantify ocean acidification and related uncertainties at a given level of global warming for different choices of greenhouse gas emission reductions remain missing.

The magnitude of ocean acidification and the associated uncertainty at a given stabilized temperature level can, however, be determined by simulations that adapt greenhouse gas emissions successively to converge to the same stabilized warming level. Such simulations prescribe the future warming level and not the atmospheric CO_2 trajectories and hence do not quantify the uncertainty of warming per increase of atmospheric CO_2 but the uncertainty of increases of atmospheric CO_2 per warming. Approaches like the Adjusting Mitigation Pathway (AMP) approach [51] or the recently developed Adaptive Emission Reduction Approach (AERA) [52] allow to make such simulations with Earth System Models by developing dynamically emission curves, which stabilize the simulated warming at any chosen temperature target. Here, we use the AERA, which accounts for all radiative agents and not only for CO_2 as the AMP, in combination with a reduced-form atmospheric chemistry model and the Earth System Model of Intermediate Complexity Bern3D-LPX with varying climate sensitives and ocean mixing rates [53,54] to quantify ocean acidification when warming stabilized at 1.5°C, 2.0°C, 2.5°C, and 3.0°C above preindustrial temperature and the uncertainty due to varying TCREs, and the choice of reductions in CO_2 and non-CO_2 GHG emission. We use different configurations of Bern3D-LPX as a surrogate for a typical CMIP ensemble of ESM. The wide range of simulations with the AERA demonstrates that the main uncertainty of ocean acidification projection for a given warming stems mainly from the uncertainty in the knowledge of TCRE and the choice in the reductions in non-CO_2 emissions. Moreover, the AERA simulations with Bern3D-LPX underline the importance of emission-driven temperature stabilization simulations in the CMIP framework for projections and uncertainty assessments of the Earth system, its carbon cycle [55], extreme events [43,56], and ecosystem stressors [19] in a stabilized climate.

2. Methods

2.1 Adaptive Emission Reduction Approach (AERA)

The AERA estimates a future trajectory of CO_2 forcing equivalent (CO_2-fe) emissions [2,3,10] that allows to stabilize the global atmospheric surface warming at a prescribed temperature level in three steps solely based on past annually averaged trajectories of (1) CO_2 emissions, (2) atmospheric CO_2, (3) the radiative forcing of all non-CO_2 forcing agents, and (4) global mean surface temperatures [52].

First, the AERA estimates the anthropogenic warming from the time series of radiative forcing and temperatures [57] using an impulse response function [58]. Second, the determined anthropogenic warming and the cumulative CO_2-fe emissions (sum of CO_2 emissions from fossil fuels and land use change and CO_2-fe from non-CO_2 radiative agents [3]) are used to determine the transient climate response to cumulative CO_2-fe emissions (TCRE) [2,3,5,8]. The TCRE then allows to estimate the remaining allowable emission budget (REB) of CO_2-fe before the chosen temperature target is reached. In the third step, the CO_2-fe in the REB are distributed over the next decades so that an overshoot in temperature is tried to be avoided and that year-to-year changes in CO_2-fe emission reductions remain as small as possible. A detailed explanation of the AERA is provided by Terhaar et al. (2022) [52].

2.2 Bern3D-LPX

Bern-3D-LPX is an Earth System Model of intermediate complexity that simulates dynamically the physics, chemistry, and biology of the land biosphere, the ocean, and sea ice, as well as their coupling to the atmosphere [59,60]. The model is used at nine different setups that cover TCREs from 1.35 °C $(EgC)^{-1}$ to 2.16 °C $(EgC)^{-1}$, which resembles the CMIP6 TCRE range of 1.32-2.30 °C $(EgC)^{-1}$ ($EgC = 1000\ PgC = 10^{18}\ gC$) [61] and the observation-constrained range of 1.3-2.3 °C $(EgC)^{-1}$ [50]. The range of TCREs is obtained by combinations of three different ocean diapycnal mixing parameters ($3e^{-5}$, $2e^{-5}$, $1e^{-5}$ $m^2\ s^{-1}$) and three different climate feedback parameters (-0.1, -0.5, -1.0 W m^{-2} K^{-1}) that account for feedbacks in the Earth System that are not explicitly or potentially not correctly simulated by Bern3D-LPX. These setups were chosen as their range of Equilibrium

Climate Sensitivities (ECS) from 2.3 to 4.6°C covers the 5-95% likelihood range of the latest ECS assessment based on multiple lines of evidence [62] and because the ocean mixing parameters result in a circulation that represents observed distributions of CFCs, O_2, or $\Delta^{14}C$ [60,63].

2.3 Simulations and non-CO_2 radiative agents

The simulations with Bern3D-LPX start in 1765 and are until 2025 all prescribed with the same CO_2 emissions, non-CO_2 radiative forcing, and land use area change. CO_2 emissions are from the Global Carbon Budget until 2020 [64] and develop from 2021 to 2025 proportionally to the national determined contributions as quantified by the Climate Action Tracker [65]. Non-CO_2 radiative forcing is based on the RCP database until 2000 [66–70] and from 2000 to 2025 on the most recent assessment from chapter 7 in the IPCC AR6 WG1 [71] report using SSP2-4.5 as an extension of the historical period after 2014 [44] to better reflect historic CH_4 and N_2O emissions over the last years. Land-use change is prescribed from 1850 to 2100 based on SSP1-2.6 [72] and associated emissions are dynamically calculated by Bern3D-LPX. SSP1-2.6 was chosen for land-use change as CMIP simulations following this scenario result in temperature are on average between 1.5°C and 2.0°C [47], the temperature targets that are closest to the aims of the Paris Agreement to limit warming well below 2°C and to pursuit efforts to reduce it to 1.5°C [1]. Volcanic radiative forcing is based on the Ice-core Volcanic Index 2 [73,74] until 2000 and zero afterwards.

From 2025 to 2300, the emissions of CO_2, N_2O, CH_4, CO, NOx, and VOC as well as trajectories of other non-CO_2 radiative agents, such as aerosols, evolve dynamically to match the prescribed CO_2-fe emission curve, which is updated every five years. The AERA is first applied in 2025 and then every five years to mimic the stocktake process foreseen in the Paris Agreement that includes a new submission of world-wide NDCs every five years with the next NDC submission being in 2025. The emissions of N_2O, CH_4, CO, NOx, and VOC are used by a reduced form atmospheric chemistry model to calculate their respective atmospheric concentrations and the associated radiative forcing and CO_2-fe emissions. A detailed explanation of the reduced atmospheric chemistry model and parameters is provided by Terhaar et al. (2022) [52]. The ozone forcing and the aerosol forcing in the atmospheric chemistry model was here changed to 0.47 W m^{-2} and -1.06 W m^{-2} in 2019, respectively, to match the non-CO_2 radiative forcing from the IPCC AR6 WG1 report [71].

As many combinations of the different GHGs and radiative agents exist that would lead to the same prescribed CO_2-fe emission curve, prior assumptions must be made for the evolution of the non-CO_2 radiative agents. Three sets of simulations were made to represent a wide range of future choices (Supplementary Table 1). In the first set of simulations, called '*baseline'*, CH_4 and N_2O emissions evolve after 2020 according to SSP2-4.5, under which global warming will likely be limited to 2°C warming [75], and CH_4 and N_2O emissions are constant from 2100 onwards (Supplementary Figure 1). Although SSP1-2.6 represents the scenario that results in temperatures closest to the Paris Agreement targets (see above), we chose SSP2-4.5 to provide a set of simulations were CO_2 reductions are relatively higher so that the three sets of simulations span a range of CO_2 emissions. In addition, the aerosol radiative forcing decreases exponentially (80% with a lifetime of 100 years, and 20% with a lifetime of 50 years). CO_2 emissions evolve dynamically so that the total CO_2-fe emission match the AERA-prescribed CO_2-fe emissions. In the second set of simulations, called '*high-CO_2*', aerosols also decrease exponentially as in the 'baseline' simulations and CH_4 and N_2O emissions evolve parallel to CO_2 emissions. The parallel evolution causes CH_4 and N_2O emissions to decrease faster than under SSP2-4.5 and result accordingly in smaller CO_2-fe emissions from CH_4 and N_2O. Reductions in CO_2 emissions can therefore be weaker to still equal the same CO_2-fe emission than in the baseline simulation, which yields comparatively higher CO_2 emissions. In the third set of simulation, called '*constant aerosol'*, CO_2, CH_4, and N_2O emissions also evolve proportionally but the aerosol radiative forcing remains at 2025 levels. Therefore, even less stringent CO_2 emission reductions are necessary in this set of simulations to reach the temperature targets and CO_2 emissions and, in turn, atmospheric CO_2 can remain higher than in the 'baseline' and 'high-CO_2' simulations. Land-use change remains unchanged across all simulations.

Throughout the manuscript, we focus on the 'baseline' and 'high-CO_2' simulations that rely only on emission reductions, which are the only sustainable to reach a prescribed temperature target [76]. As opposed to these mitigation scenarios, the '*constant aerosol'* simulations also rely on strong aerosol injection via solar radiation modification to keep the aerosol forcing constant. Solar radiation modification is only an emergency solution as it comes with high risks, e.g., an abrupt rise in temperatures if the solar radiation modification should fail in the future for technical or political reasons [77], further commitments and unintended side effects like shifting monsoon patterns, changes in meridional temperature gradients, atmospheric and oceanic circulation, and the modes of climate variability [78]. By presenting solar radiation modification briefly in the main manuscript we transparently show all theoretical options but focus on the sustainable and more likely options.

In all simulation, CH_4 and N_2O emissions have lower limits of 30 Tg CH_4 yr^{-1} and 5.3 Tg N_2O yr^{-1} due to non-abatable emissions in agriculture and livestock sectors. Simulations for the three set of simulations were made for four temperature targets of 1.5°C, 2.0°C, 2.5°C, and 3.0°C with each of the nine setups of Bern3D-LPX representing ECS' from 2.3 to 4.7°C, resulting in 108 simulations (3 set of simulations x 4 temperature targets x 9 Bern3D-LPX setups). As Bern3D-LPX underestimates the inter-annual variability, each of these 108 setups was made with eight temporally varying superimposed inter-annual surface atmospheric temperature variabilities that are derived from observations [52] and hence yield 864 simulations in total (3 set of simulations x 4 temperature targets x 9 Bern3D-LPX setups x 8 temperature variabilities; Supplementary Table 1).

As all setups with different ECS simulate a different historical warming until 2020 compared to the 1850-1900 period (0.83-1.39°C), the remaining emissions and increases in atmospheric CO_2 until a chosen temperature target is reached depends sensitively on this past warming. To remove this uncertainty, the temperature target is always defined relative to the observation-based anthropogenic warming in year 2020, which is estimated to be 1.23±0.20°C [52]. For the 1.5°C target, this means that an allowable warming of 0.27°C remains. This allowable warming is then added to the anthropogenic warming in each setup. This Δ-approach is the same that is regularly used for ocean acidification studies where different models have difficulties to simulate the baseline biogeochemistry in the interior ocean at present [23,37,39,40].

3. The carbon cycle and ocean acidification in a stabilized 1.5°C world

3.1 Uncertainty from the transient climate response to cumulative carbon emissions

The simulated historical temperature anomaly with respect to 1850-1900 under prescribed CO_2 emissions increases at a similar pace as the observed temperature over all nine model setups (±0.25°C), despite varying climate sensitivities and ocean carbon sink strengths (Figure 1a). All model setups do not only capture the historical temperature trajectory, but also the observed trajectory of atmospheric CO_2 [79] (Figure 1d), the observation-based estimate of the cumulative ocean carbon uptake [64] (Figure 1e), and the globally averaged pH over the last decades (Figure 1f).

After the AERA is switched on in 2025, all trajectories converge by 2150 within ±0.05°C to the prescribed 1.5°C temperature target because fossil fuel CO_2 emissions evolve freely so that the combined CO_2-fe emissions from fossil fuels, land use change, and non-CO_2 radiative agents match the prescribed CO_2-fe emissions by the AERA. The total CO_2-fe emissions from 2021 to 2150 that allow to meet the 1.5° target vary from -59 Pg C to +203 Pg C (range of nine setups after averaging over all eight realizations with varying inter-annual superimposed variability) under the 'baseline' scenario (Figure 1b). The uncertainty ranges (-35 Pg C to +239 Pg C under the 'high-CO_2' scenario; -27 Pg C to +255 Pg C under the 'constant aerosol' scenario) differ between the three scenarios due to the good but imperfect transformation of non-CO_2 radiative forcing to CO_2-fe emissions. In simulations with the AERA that converge to a temperature target, the uncertainty from the TCRE transfers into the CO_2-fe budget, whereas traditional projections used in the IPCC reports [47] based on Shared Socioeconomic Pathways (SSPs) [44,45,80] have an inter-model temperature range for a given CO_2-fe trajectory (for example, the 5-95% range for global warming in 2100 under SSP1-2.6 is 1.3-2.8°C) [47].

The range of cumulative CO_2-fe emissions from 2021 to 2150 that allow to meet the 1.5°C target (-59 Pg C to +203 Pg C for the 'baseline' scenario) propagates directly into different fossil fuel CO_2 emission trajectories. The remaining allowable fossil fuel CO_2 emissions depend on AERA derived CO_2-fe emissions and the non-CO_2 emissions and the CO_2 emissions from land-use change. In the 'baseline' scenario, CH_4 and N_2O emissions and aerosols follow prescribed trajectories, resulting in CO_2-fe emissions of all non-CO_2 radiative agents from 2021 to 2150 of 160 Pg C and land-use change emissions of 17 Pg C.

Therefore, the remaining allowable fossil-fuel CO_2 emissions from 2021 to 2150 under this scenario range from -236 Pg C to +25 Pg C (Figure 1c).

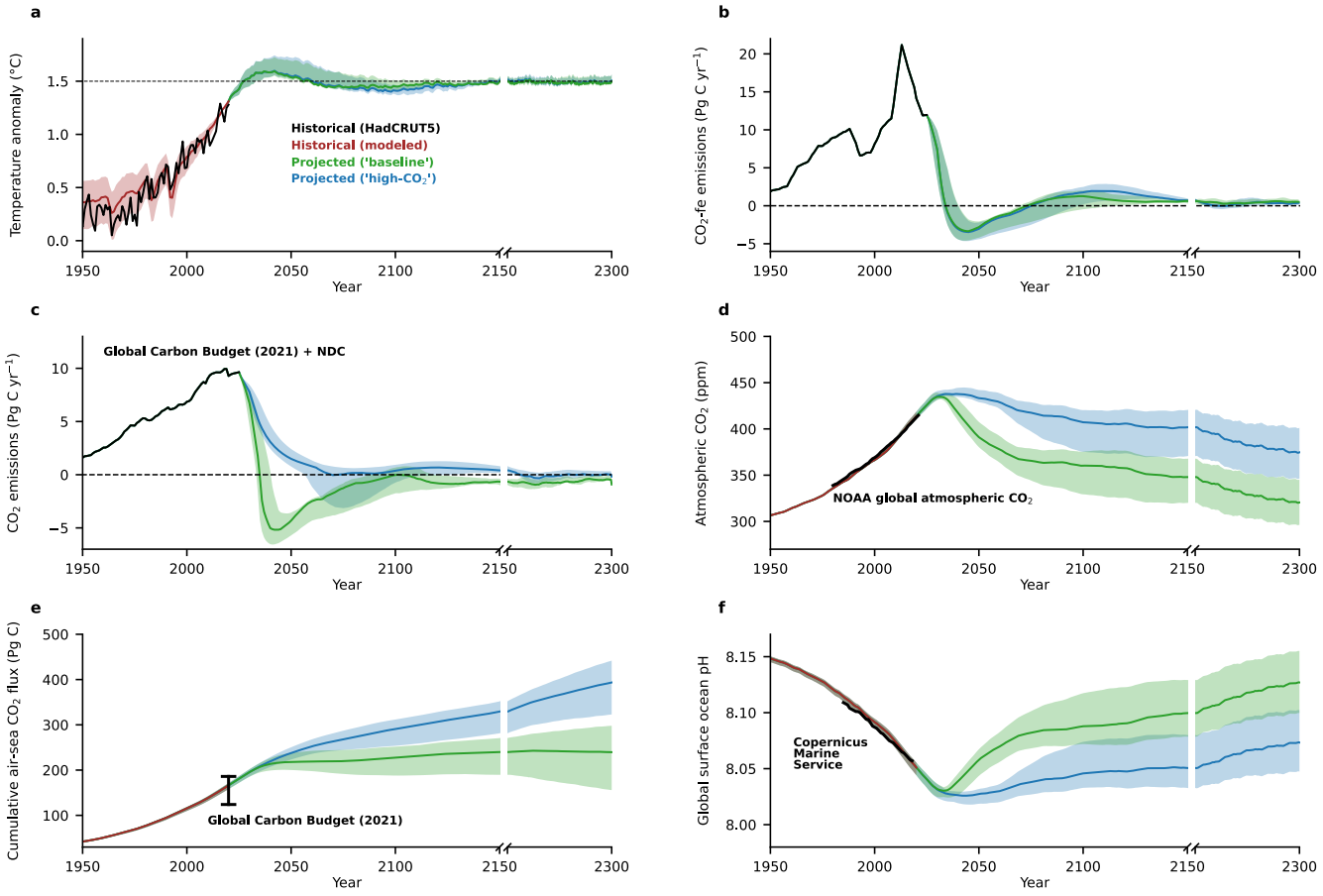

Figure 1. Temperature anomalies, associated CO_2 forcing equivalent emissions, and carbon cycle dynamics. a) Global mean surface temperature anomalies over the historical period until 2020 as observed by HadCRUT5 [81] (black line) and as simulated by the Bern3D-LPX (brown). After 2020, projections are shown for the 1.5°C target for the 'baseline' (green) and high-CO_2 (blue) scenarios. The dashed black line shows the 1.5°C temperature target. **b)** CO_2 forcing equivalent (CO_2-fe) emissions and **c)** CO_2 emissions as prescribed from the Global Carbon Budget 2021 [64] and NDCs until 2025 (black) and adaptively developed by the AERA from 2025 onwards. The dashed lines represent zero emissions. Simulated **d)** atmospheric CO_2, **e)** cumulative air-sea CO_2 flux since 1765 (annual air-sea CO_2 fluxes are shown in Supplementary Figure 2), and **f)** globally averaged surface ocean pH. The green and blue lines indicate simulations with the model setup that has an ECS of 3.2°C, the central estimate according to Sherwood et al. (2020) [62]. The shading indicates the range of all model setups with ECS' from 2.3 to 4.7°C (5-95% ECS likelihood range) [62]. In addition, observation-based estimates of the **d)** past global atmospheric CO_2 from NOAA averaged over marine surface sites [79], the **e)** historical cumulative ocean carbon uptake from the Global Carbon Budget 2021 [64], and the **f)** past global surface average pH from the Copernicus Marine Service (https://doi.org/10.48670/moi-00047) is shown.

The range of CO_2 emission trajectories affects the projected atmospheric CO_2 and the rates and magnitude of ocean carbon uptake (Figure 1d-e, Supplementary Figure S2). By 2150, possible atmospheric CO_2 in a 1.5°C world under the 'baseline' scenario range from 320 ppm to 368 ppm after having peaked at 433 to 439 ppm between 2030 and 2035, and the cumulative ocean carbon sink from 1765 to 2150 varies from 190 Pg C to 271 Pg C. In comparison, the SSPs that are used by the IPCC have by definition no uncertainty in the future atmospheric CO_2 as atmospheric CO_2 is prescribed as a boundary condition. While the uncertainty of the atmospheric CO_2 in 2100 is by definition non-existent, the range of the cumulative carbon sink is also smaller when atmospheric CO_2 is prescribed, for example 274-332 Pg C for SSP1-2.6 across the CMIP6 ensemble [55]. Thus, when CO_2 emissions evolve freely to converge to a temperature target, the range of the future sink is ~40% larger than under fixed atmospheric CO_2.

The wide range of possible atmospheric CO_2 translates into different surface ocean pH projections. At the ocean surface changes in pH are almost entirely driven by changing dissolved inorganic carbon [56], which in turn closely follows the changes in atmospheric CO_2 due to the air-sea CO_2 flux that tends to equilibrate differences in CO_2 partial pressure between the atmosphere and ocean. Hence, the projected atmospheric CO_2 range from 320 ppm to 368 ppm in 2150 results in an almost perfectly anti-correlated projected range in surface ocean pH from 8.079 to 8.129 (after a minimum of 8.024-8.033 between 2031 and 2037) (Figures 1d and 1f). This range is an order of magnitude larger than the projected standard deviation in projected ocean surface pH of ±0.002 under SSP1-2.6 in 2100 [19]. Furthermore, the annually averaged surface area that is projected to have saturation states of aragonite – a mineral form of calcium carbonate produced by marine organisms – below one remains almost non-existent ($<10^6$ km^2) due to the rapidly decreasing CO_2 emissions. However, saturation states may still drop below one on diurnal [82,83] or seasonal [31,84] timescales or in the 126 meters below the surface (Figure 3f, Supplementary Figure 3), where calcifying organisms vertically migrate [85].

As opposed to surface ocean acidification, long-term ocean acidification below the surface depends not only on the increasing surface ocean dissolved inorganic carbon but also on the quantity of additional dissolved inorganic carbon at the ocean surface that is transported below the ocean surface [31,37,39,40,55,86] and distributed within the ocean [42,87]. The decrease in the global ocean volume that is projected to remain saturated towards aragonite ($\Omega_A > 1$) from 2002 to 2150 ranges from 47 to 86 x 10^6 km^3 (17-32 % of supersaturated volume in 2002) (Figure 2a), with the central estimate (setup with ECS=3.2°C) being 71 x 10^6 km^3 (26%) and the standard deviation across all nine setups being 12 x 10^6 km^3 (4%). Similarly, the range in volumes changes with Ω_A between 1 and 2, 2 and 3, and above 3 vary strongly across the different model setups.

Under prescribed atmospheric CO_2 in SSP1-2.6, the simulated decrease in volume that is projected to remain saturated towards aragonite (Ω_A >1) in 2100 is 89±6 x 10^6 km^3 [55]. Thus, the uncertainty of future interior ocean acidification rates under a prescribed temperature target when using the AERA is around twice as large as under prescribed atmospheric CO_2. The difference in uncertainty under prescribed temperature targets and prescribed atmospheric CO_2 is smaller in the ocean interior (factor 2) than at the ocean surface (factor 10), because most water masses are not in direct contact with the atmosphere so that the differences in simulated ocean circulation and deep-water formation affects both kinds of simulations [37,39,40,55,88,89].

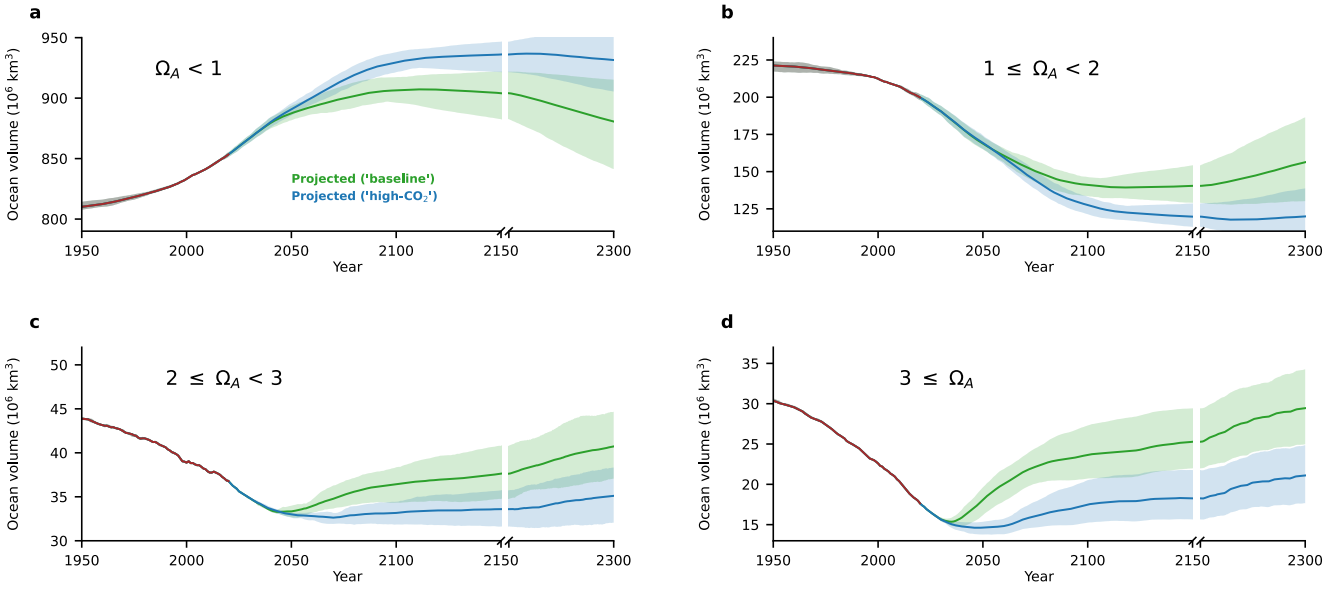

Figure 2. Interior ocean aragonite saturation state over time. Global mean ocean volume of water masses with aragonite saturation states **a)** below 1, **b)** between 1 and 2, **c)** between 2 and 3, and **d)** above 3 as simulated by the Bern3D-LPX until 2020 (brown) and from 2020 to 2300 for the 1.5°C target under the 'baseline' (green) and 'high-CO_2' (blue) scenario. The lines indicate simulations with the model setup that has an ECS of 3.2, the central estimate according to Sherwood et al. (2020) [62]. The shading indicates the range of all model setups with ECSs from 2.3 to 4.7°C (5-95% ECS likelihood range [62]). Saturation states in 2002 are calculated from observation-based global ocean estimates of dissolved inorganic carbon, alkalinity, temperature, salinity, silicon, and phosphorus from GLODAPv2 [90]. For all other years, saturation states are calculated from the observation-based dissolved inorganic carbon, alkalinity, temperature, salinity, silicon, and phosphorus in 2002 plus the respective simulated changes in with respect to 2002 [23,37,40]. The same timeseries for the upper 126 m are shown in Supplementary Figure 3.

3.2 Uncertainty from the choice of reductions of non-CO_2 radiative agents

The evolution of non-CO_2 radiative forcing agents does not influence the temperature and CO_2-fe trajectory (Figure 1a,b) but limits, for a given temperature target, the range of possible future trajectories of CO_2 emissions, atmospheric CO_2 , ocean carbon uptake, surface ocean pH, and interior ocean aragonite saturation states (Figures 1c-f, 2). Under the 'baseline' scenario, non-CO_2 radiative agents are prescribed following SSP2-4.5 and the radiative forcing of major non-CO_2 radiative agents (N_2O, CH_4, and aerosols) under SSP2-4.5 do not get strongly reduced. Thus, the reduction in CO_2-fe emissions as prescribed by the AERA is achieved via reductions in CO_2 emissions. As opposed to the 'baseline' scenario, the radiative forcing or emissions of the major non-CO_2 radiative agents are reduced strongly under the 'high-CO_2' scenario so that CO_2 emissions remain higher from 2025 to 2075, yielding a remaining CO_2 budget from 2021 to 2150 of 54 to 286 Pg C, significantly larger than the -236 Pg C to +25 Pg C range under the 'baseline' scenario. As CO_2 emissions are larger under the 'high-CO_2' scenario, so are atmospheric CO_2 (371-420 ppm in 2150 after having peaked at 436-445 ppm between 2034 and 2043), and the cumulative carbon uptake by the ocean (281-352 Pg C in 2150).

The larger atmospheric CO_2 in the 'high-CO_2' scenario and the larger cumulative carbon uptake by the ocean result in higher ocean acidification. The range of projected surface ocean pH across the nine different model setups with stronger reduction in non-CO_2 radiative agents is 8.033-8.080 in 2150 (after a minimum of 8.018-8.029 between 2042 and 2047) (Figures 1d and 1f). The decrease in volume that is projected to remain saturated towards aragonite ($\Omega_A > 1$) in 2150 under the 'high-CO_2' scenario ranges from 86 to 111 x 10^6 km^3 (31-41 %) (Figure 2a). Overall, the choice of non-CO_2 radiative forcing agents hence increases the possible range of ocean acidification rates in a 1.5°C world by a factor of two and makes the uncertainty about the future ocean acidification rates in a 1.5°C world thus even larger than it already was due to the different TCRE's (see above). The entire range of globally averaged surface ocean pH under both scenarios of 0.096 is thus as large as the difference in surface ocean pH between SSP1-2.6 (warming of 1.3-2.8°C [47]) and SSP2-4.5 (warming of 2.1-4.0°C) and ~50 times as large as the inter-model difference for each scenario across the range of CMIP6 Earth System Models [19].

In addition to the 'high-CO_2' scenario, the 'constant aerosol' scenario allows to assess a potential future in which the necessary greenhouse gas reductions are compensated by continuing aerosol emissions so that the cooling effect of aerosols in the atmosphere does not reduce over the 21st century. In that scenario, the CO_2 emissions can remain even higher, yielding higher atmospheric CO_2 in 2150 (411-465 ppm), higher ocean cumulative CO_2 uptake from 1765 to 2150 (335-405 Pg C), and

much more severe ocean acidification with globally averaged pH values in 2150 ranging from 7.998 to 8.045 (Supplementary Figure 4). This example demonstrates the importance of multiple climate targets [17] in addition to temperature targets to reduce the damaging effect of anthropogenic emissions on Earth ecosystems.

4. The carbon cycle and ocean acidification if global warming permanently exceeds the temperature targets of the Paris Agreements

The Paris Agreement aims at limiting global warming well below 2°C and reducing it to 1.5°C [1]. However, recent carbon and non-CO_2 greenhouse gas emissions suggest that this target may not be met [65,91]. Hence, it is important to quantify the effect of different warming levels that permanently overshoot the Paris Agreement temperature goals on the carbon cycle and ocean acidification. In this section, the projected atmospheric CO_2, ocean carbon uptake, surface ocean pH, and interior ocean Ω_A are quantified for a 2.0°C, 2.5°C, and 3.0°C target (Figure 3, Supplementary Table 2) although many other targets would be possible.

With increasing warming, the range across setups increases as the transient climate response to cumulative emissions (TCRE) leads to a higher range in the remaining emission budget for a higher temperature target. In 2150, when the temperature stabilizes in these simulations, the higher range in the remaining emission results in large uncertainty ranges in past cumulative CO_2 emissions and ocean carbon uptake, as well as large ranges in atmospheric CO_2, surface ocean pH, and the volume of water undersaturated towards aragonite are simulated across the different model setups. These ranges even overlap for different temperature targets. Under the 'baseline' scenario, even the projections for the 2.0°C and 3.0°C target almost overlap. When adding uncertainties from the choice of the non-CO_2 emissions, the projections of the 2.0°C and 3.0°C targets overlap strongly. Furthermore, the differences between the projections of the carbon cycle between the 'baseline' and 'high-CO_2' are reduced under higher temperature targets because non-CO_2 emissions under the 'high-CO_2' are proportional to CO_2 emissions. As CO_2 emissions remain higher for a warmer temperature target so are the emissions of non-CO_2 radiative agents, which remain hence closer to the prescribed emissions of non-CO_2 radiative agents under the 'baseline' scenario.

Overall, the comparison demonstrates the large uncertainties of the carbon cycle projections under prescribed temperature targets, which are not apparent under usual projections by Earth System Models under RCPs or SSPs with prescribed trajectories of atmospheric CO_2 and non-CO_2 radiative agents.

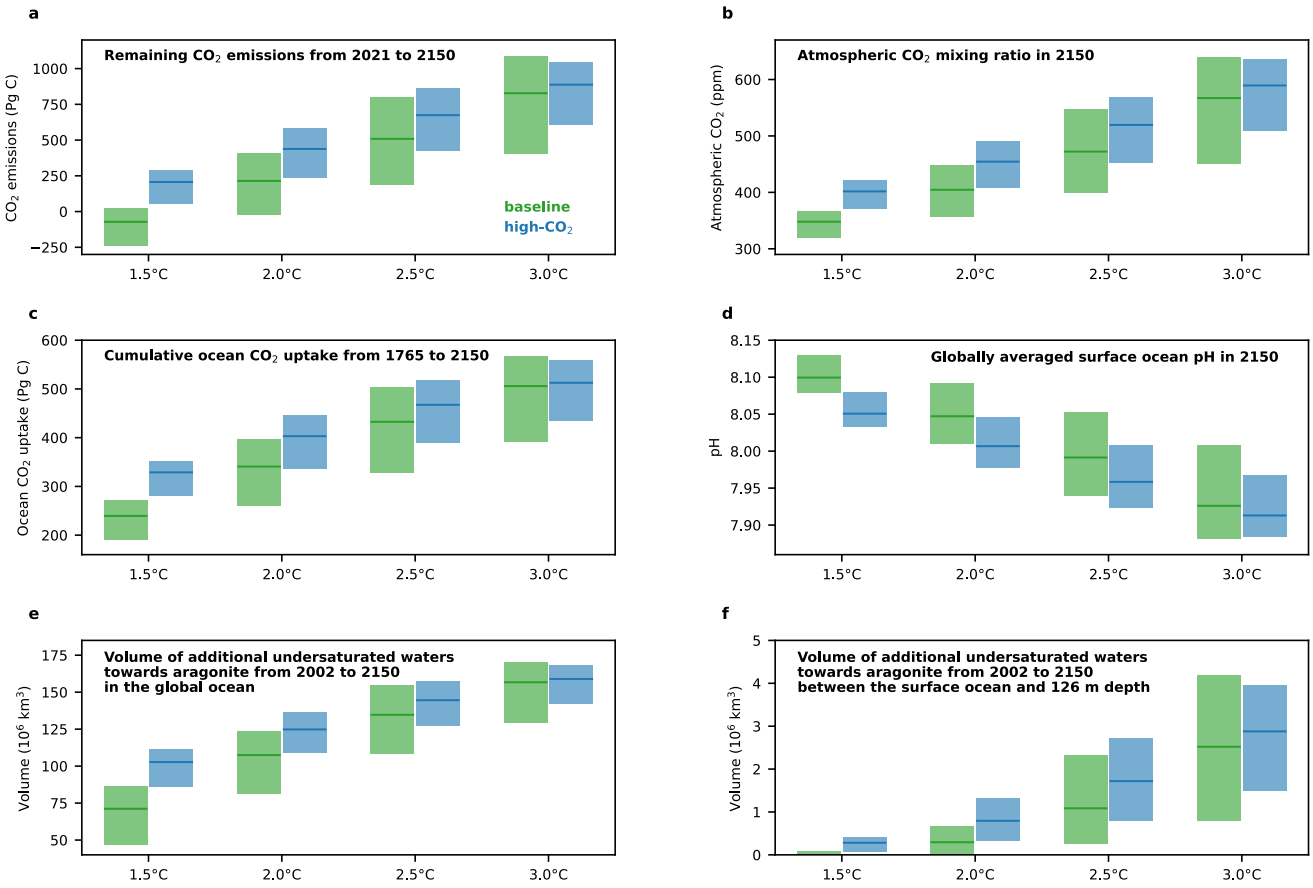

Figure 3. Projected carbon cycle and ocean acidification under various temperature targets. a) Remaining CO_2 emissions from 2021 to 2150 that allow meeting the temperature targets, **b)** atmospheric CO_2 in 2150, **c)** cumulative ocean carbon uptake from 1765 to 2150, **d)** globally averaged surface ocean pH in 2150, and **e)** the additionally undersaturated waters towards aragonite from 2002 to 2150 for the 'baseline' (blue) and 'high-CO_2' (blue) scenarios for stabilized warming at 1.5°C, 2.0°C, 2.5°C, and 3.0°C for the entire ocean and **f)** only for the upper 126 m below the surface. The thick lines represent the model setups that has an ECS of 3.2°C, the central estimate according to Sherwood et al. (2020) [62]. The colored shading indicates the range across all nine setups. All results were averaged across the eight realizations of each setup with varying superimposed inter-annual variability.

5. Conclusion

The simulations with the AERA allow assessing the so-far unknown uncertainties of the ocean carbon cycle and ocean acidification under prescribed temperature targets. Until now, future ocean acidification was assessed by the IPCC [33] and other studies [18,19] using scenarios with prescribed atmospheric CO_2 trajectories [18,19,33] and only few studies assessed uncertainties in acidification metrics by prescribing or remapping carbon emissions [49,50]. The uncertainties for global and regional ocean acidification projections under prescribed atmospheric CO_2 trajectories were reduced with great efforts by understanding differences between the different Earth System Models [37,39,40,55]. However, here we show that the uncertainties stemming from the TCRE, which is determined by the Earth's warming response to greenhouse gases, e.g., ECS, and ocean carbon uptake, are twice as large to a magnitude larger than the inter-model differences in the usual projections.

The here provided simulations are made with an Earth System Model of intermediate complexity and provide robust projections of the globally or basin-wide averaged projections. For projections of ocean acidification on a regional scale like the Gulf of Alaska [92], the Eastern Boundary upwelling systems [93,94], the Arctic Ocean [37,40], or the Southern Ocean [39,87], state-of-the-art Earth System Models representing small scale circulation [42,95–97] would need to be run with the AERA in the future.

The difference in the projected future of the ocean carbon uptake and ocean acidification also highlights the importance of the choice of emission reductions between CO_2 and non-CO_2 emissions for the ocean ecosystems that are vulnerable to ocean acidification. While many different combinations of reductions in CO_2 and non-CO_2 emissions allow reaching a given temperature target, these different combinations may affect ecosystems vulnerable to ocean acidification in very different ways. In the case of ocean acidification, the same amount of CO_2-fe emissions in form of CO_2 emissions is more harmful to the ocean than in form of N_2O or CH_4 emissions. Moreover, the possible implementation of solar radiation modification, e.g., via continuing aerosol emissions, to limit global warming to 1.5°C would still cause high ocean acidification rates. Hence, when agreeing on climate targets policy makers should not only focus on warming levels [1], but also on other climate targets [17].

Acknowledgements

This work was funded by the European Union's Horizon 2020 research and innovation program under grant agreement no. 821003 (project 4C, Climate–Carbon Interactions in the Current Century) (Jens Terhaar, Thomas L. Frölicher, Fortunat Joos) no. 820989 (project COMFORT, Our common future ocean in the Earth system-quantifying coupled cycles of carbon, oxygen and nutrients for determining and achieving safe operating spaces with respect to tipping points) (Thomas L. Frölicher, Fortunat Joos), and no. 101003687 (project PROVIDE, Paris Agreement Overshooting) (Thomas L. Frölicher) as well as by Woods Hole Oceanographic Institution Postdoctoral Scholar Program (Jens Terhaar), and the Swiss National Science Foundation under grant PP00P2_198897 (Thomas L. Frölicher) and grant #200020_200511 (Jens Terhaar, Fortunat Joos). This study has been conducted using E.U. Copernicus Marine Service Information; https://doi.org/10.48670/moi-00047. The work reflects only the authors' view; the European Commission and their executive agency are not responsible for any use that may be made of the information the work contains.

Author contributions

JT, TLF, and FJ are responsible for conceptualization and methodology. JT made the simulations, analyses, visualization, and wrote the original draft. TLF and FJ were responsible for funding acquisition. TLF and FJ were responsible for project administration. JT, TLF, and FJ were responsible for writing, review, and editing.

Competing interests

The contact author has declared that none of the authors has any competing interests.

References

[1] UNFCCC 2015 *Paris agreement. Report of the Conference of the Parties to the United Nations Framework Convention on Climate Change* (Paris)

[2] Jenkins S, Millar R J, Leach N and Allen M R 2018 Framing Climate Goals in Terms of Cumulative CO2-Forcing-Equivalent Emissions *Geophys. Res. Lett.* **45** 2795–804

[3] Smith M A, Cain M and Allen M R 2021 Further improvement of warming-equivalent emissions calculation *npj Clim. Atmos. Sci.* **4** 19

[4] Matthews H D and Caldeira K 2008 Stabilizing climate requires near-zero emissions *Geophys. Res. Lett.* **35**

[5] Matthews H D, Gillett N P, Stott P A and Zickfeld K 2009 The proportionality of global warming to cumulative carbon emissions *Nature* **459** 829–32

[6] Allen M R, Frame D J, Huntingford C, Jones C D, Lowe J A, Meinshausen M and Meinshausen N 2009 Warming caused by cumulative carbon emissions towards the trillionth tonne *Nature* **458** 1163–6

[7] MacDougall A H, Frölicher T L, Jones C D, Rogelj J, Matthews H D, Zickfeld K, Arora V K, Barrett N J, Brovkin V, Burger F A, Eby M, Eliseev A V, Hajima T, Holden P B, Jeltsch-Thömmes A, Koven C, Mengis N, Menviel L, Michou M, Mokhov I I, Oka A, Schwinger J, Séférian R, Shaffer G, Sokolov A, Tachiiri K, Tjiputra J, Wiltshire A and Ziehn T 2020 Is there warming in the pipeline? A multi-model analysis of the Zero Emissions Commitment from CO_2 *Biogeosciences* **17** 2987–3016

[8] Zickfeld K, Eby M, Matthews H D and Weaver A J 2009 Setting cumulative emissions targets to reduce the risk of dangerous climate change *Proc.*

Natl. Acad. Sci. **106** 16129

[9] Zickfeld K, MacDougall A H and Matthews H D 2016 On the proportionality between global temperature change and cumulative CO 2 emissions during periods of net negative CO 2 emissions *Environ. Res. Lett.* **11** 055006

[10] Allen M R, Shine K P, Fuglestvedt J S, Millar R J, Cain M, Frame D J and Macey A H 2018 A solution to the misrepresentations of CO2-equivalent emissions of short-lived climate pollutants under ambitious mitigation *npj Clim. Atmos. Sci.* **1** 16

[11] Damon Matthews H, Tokarska K B, Rogelj J, Smith C J, MacDougall A H, Haustein K, Mengis N, Sippel S, Forster P M and Knutti R 2021 An integrated approach to quantifying uncertainties in the remaining carbon budget *Commun. Earth Environ.* **2** 7

[12] Rogelj J, Forster P M, Kriegler E, Smith C J and Séférian R 2019 Estimating and tracking the remaining carbon budget for stringent climate targets *Nature* **571** 335–42

[13] Tokarska K B, Zickfeld K and Rogelj J 2019 Path Independence of Carbon Budgets When Meeting a Stringent Global Mean Temperature Target After an Overshoot *Earth's Futur.* **7** 1283–95

[14] Jones C D and Friedlingstein P 2020 Quantifying process-level uncertainty contributions to TCRE and carbon budgets for meeting Paris Agreement climate targets *Environ. Res. Lett.* **15** 074019

[15] Peters G P 2018 Beyond carbon budgets *Nat. Geosci.* **11** 378–80

[16] Matthews H D, Tokarska K B, Nicholls Z R J, Rogelj J, Canadell J G, Friedlingstein P, Frölicher T L, Forster P M, Gillett N P, Ilyina T, Jackson R B, Jones C D, Koven C, Knutti R, MacDougall A H, Meinshausen M, Mengis N, Séférian R and Zickfeld K 2020 Opportunities and challenges in using remaining carbon budgets to guide climate policy *Nat. Geosci.* **13** 769–79

[17] Steinacher M, Joos F and Stocker T F 2013 Allowable carbon emissions lowered by multiple climate targets *Nature* **499** 197–201

[18] Bopp L, Resplandy L, Orr J C, Doney S C, Dunne J P, Gehlen M, Halloran P, Heinze C, Ilyina T, Séférian R, Tjiputra J and Vichi M 2013 Multiple stressors of ocean ecosystems in the 21st century: projections with CMIP5 models *Biogeosciences* **10** 6225–45

[19] Kwiatkowski L, Torres O, Bopp L, Aumont O, Chamberlain M, Christian J R, Dunne J P, Gehlen M, Ilyina T, John J G, Lenton A, Li H, Lovenduski N S, Orr J C, Palmieri J, Santana-Falcón Y, Schwinger J, Séférian R, Stock C A, Tagliabue A, Takano Y, Tjiputra J, Toyama K, Tsujino H, Watanabe M, Yamamoto A, Yool A and Ziehn T 2020 Twenty-first century ocean warming, acidification, deoxygenation, and upper-ocean nutrient and primary production decline from CMIP6 model projections *Biogeosciences* **17** 3439–70

[20] Boyd P W and Brown C J 2015 Modes of interactions between environmental drivers and marine biota *Front. Mar. Sci.* **2** 9

[21] Kroeker K J, Kordas R L, Crim R N and Singh G G 2010 Meta-analysis reveals negative yet variable effects of ocean acidification on marine organisms *Ecol. Lett.* **13** 1419–34

[22] Doney S C, Busch D S, Cooley S R and Kroeker K J 2020 The Impacts of Ocean Acidification on Marine Ecosystems and Reliant Human Communities *Annu. Rev. Environ. Resour.* **45** 83–112

[23] Orr J C, Fabry V J, Aumont O, Bopp L, Doney S C, Feely R A, Gnanadesikan A, Gruber N, Ishida A, Joos F, Key R M, Lindsay K, Maier-Reimer E, Matear R, Monfray P, Mouchet A, Najjar R G, Plattner G-K, Rodgers K B, Sabine C L, Sarmiento J L, Schlitzer R, Slater R D, Totterdell I J, Weirig M-F, Yamanaka Y and Yool A 2005 Anthropogenic ocean acidification over the twenty-first century and its impact on calcifying organisms *Nature* **437** 681–6

[24] Gattuso J-P and Hansson L 2011 *Ocean acidification* (Oxford University Press)

[25] Kroeker K J, Kordas R L, Crim R, Hendriks I E, Ramajo L, Singh G S, Duarte C M and Gattuso J-P 2013 Impacts of ocean acidification on marine organisms: quantifying sensitivities and interaction with warming *Glob. Chang. Biol.* **19** 1884–96

[26] Kawaguchi S, Ishida A, King R, Raymond B, Waller N, Constable A, Nicol S, Wakita M and Ishimatsu A 2013 Risk maps for Antarctic krill under projected Southern Ocean acidification *Nat. Clim. Chang.* **3** 843–7

[27] Albright R, Caldeira L, Hosfelt J, Kwiatkowski L, Maclaren J K, Mason B M, Nebuchina Y, Ninokawa A, Pongratz J, Ricke K L, Rivlin T, Schneider K, Sesboüé M, Shamberger K, Silverman J, Wolfe K, Zhu K and Caldeira K 2016 Reversal of ocean acidification enhances net coral reef calcification *Nature* **531** 362–5

[28] Fabry V J, Seibel B A, Feely R A and Orr J C 2008 Impacts of ocean acidification on marine fauna and ecosystem processes *ICES J. Mar. Sci.* **65** 414–32

[29] AMAP 2013 *AMAP Assessment 2013: Arctic Ocean Acidification* (Arctic Monitoring and Assessment Programme (AMAP))

[30] Riebesell U, Gattuso J-P, Thingstad T F and Middelburg J J 2013 Preface "Arctic ocean acidification: pelagic ecosystem and biogeochemical responses during a mesocosm study" *Biogeosciences* **10** 5619–26

[31] Steinacher M, Joos F, Frölicher T L, Plattner G-K and Doney S C 2009 Imminent ocean acidification in the Arctic projected with the NCAR global coupled carbon cycle-climate model *Biogeosciences* **6** 515–33

[32] Orr J C, Kwiatkowski L and Pörtner H-O 2022 Arctic Ocean annual high in $${{\boldsymbol{p}}}_{{{\bf{CO}}}}_{{\bf{2}}}}$$could shift from winter to summer *Nature* **610** 94–100

[33] Canadell J G, Monteiro P M S, Costa M H, da Cunha L C, Cox P M, Eliseev A V, Henson S, Ishii M, Jaccard S, Koven C, Lohila A, Patra P K, Piao S, Rogelj J, Syampungani S, Zaehle S and Zickfeld K 2021 Global Carbon and other Biogeochemical Cycles and Feedbacks ed V Masson-Delmotte, P Zhai, A Pirani, S L Connors, C Péan, S Berger, N Caud, Y Chen, L Goldfarb, M I Gomis, M Huang, K Leitzell, E Lonnoy, J B R Matthews, T K Maycock, T Waterfield, O Yelekçi, R Yu and B Zhou *Clim. Chang. 2021 Phys. Sci. Basis. Contrib. Work. Gr. I to Sixth Assess. Rep. Intergov. Panel Clim. Chang.*

[34] Duarte C M, Hendriks I E, Moore T S, Olsen Y S, Steckbauer A, Ramajo L, Carstensen J, Trotter J A and McCulloch M 2013 Is Ocean Acidification an Open-Ocean Syndrome? Understanding Anthropogenic Impacts on Seawater pH *Estuaries and Coasts* **36** 221–36

[35] Tank S E, Raymond P A, Striegl R G, McClelland J W, Holmes R M, Fiske G J and Peterson B J 2012 A land-to-ocean perspective on the magnitude, source and implication of DIC flux from major Arctic rivers to the Arctic Ocean *Global Biogeochem. Cycles* **26**

[36] Terhaar J, Orr J C, Ethé C, Regnier P and Bopp L 2019 Simulated Arctic Ocean Response to Doubling of Riverine Carbon and Nutrient Delivery *Global Biogeochem. Cycles* **33** 1048–70

[37] Terhaar J, Torres O, Bourgeois T and Kwiatkowski L 2021 Arctic Ocean acidification over the 21st century co-driven by anthropogenic carbon increases and freshening in the CMIP6 model ensemble *Biogeosciences* **18** 2221–40

[38] Woosley R J and Millero F J 2020 Freshening of the western Arctic negates anthropogenic carbon uptake potential *Limnol. Oceanogr.* **65** 1834–46

[39] Terhaar J, Frölicher T and Joos F 2021 Southern Ocean anthropogenic carbon sink constrained by sea surface salinity *Sci. Adv.* **7** 5964–92

[40] Terhaar J, Kwiatkowski L and Bopp L 2020 Emergent constraint on Arctic Ocean acidification in the twenty-first century *Nature* **582** 379–83

[41] Chierici M and Fransson A 2009 Calcium carbonate saturation in the surface water of the Arctic Ocean: undersaturation in freshwater influenced shelves *Biogeosciences* **6** 2421–31

[42] Terhaar J, Orr J C, Gehlen M, Ethé C and Bopp L 2019 Model constraints on the anthropogenic carbon budget of the Arctic Ocean *Biogeosciences* **16** 2343–67

[43] Burger F A, John J G and Frölicher T L 2020 Increase in ocean acidity variability and extremes under increasing atmospheric CO_2 *Biogeosciences* **17** 4633–62

[44] Riahi K, van Vuuren D P, Kriegler E, Edmonds J, O'Neill B C, Fujimori S, Bauer N, Calvin K, Dellink R, Fricko O, Lutz W, Popp A, Cuaresma J C, KC S, Leimbach M, Jiang L, Kram T, Rao S, Emmerling J, Ebi K, Hasegawa T, Havlik P, Humpenöder F, Da Silva L A, Smith S, Stehfest E, Bosetti V, Eom J, Gernaat D, Masui T, Rogelj J, Strefler J, Drouet L, Krey V, Luderer G, Harmsen M, Takahashi K, Baumstark L, Doelman J C, Kainuma M, Klimont Z, Marangoni G, Lotze-Campen H, Obersteiner M, Tabeau A and Tavoni M 2017 The Shared Socioeconomic Pathways and their energy, land use, and greenhouse gas emissions implications: An overview *Glob. Environ. Chang.* **42** 153–68

[45] O'Neill B C, Tebaldi C, van Vuuren D P, Eyring V, Friedlingstein P, Hurtt G, Knutti R, Kriegler E, Lamarque J-F, Lowe J, Meehl G A, Moss R, Riahi K and Sanderson B M 2016 The Scenario Model Intercomparison Project (ScenarioMIP) for CMIP6 *Geosci. Model Dev.* **9** 3461–82

[46] IPCC 2013 Summary for Policymakers *Climate Change 2013: The Physical Science Basis.Contribution of Working Group I to the Fifth Assessment Report of the Intergovernmental Panel on Climate Change* ed T F Stocker, D Qin, G-K Plattner, M Tignor, S K Allen, J Boschung, A Nauels, Y Xia, V Bex and P M Midgley (Cambridge, United Kingdom and New York, NY, USA: Cambridge University Press)

[47] IPCC 2021 Summary for Policymakers *Climate Change 2021: The Physical Science Basis. Contribution of Working Group I to the Sixth Assessment Report of the Intergovernmental Panel on Climate Change* ed V Masson-Delmotte, P Zhai, A Pirani, S L Connors, C Péan, S Berger, N Caud, Y Chen, L Goldfarb, M I Gomis, M Huang, K Leitzell, E Lonnoy, J B R Matthews, T K Maycock, T Waterfield, O Yelekçi, R Yu and B Zhou (Cambridge University Press)

[48] Frölicher T L, Rodgers K B, Stock C A and Cheung W W L 2016 Sources of uncertainties in 21st century projections of potential ocean ecosystem stressors *Global Biogeochem. Cycles* **30** 1224–43

[49] Joos F, Frölicher T L, Steinacher M and Plattner G-K 2011 Impact of climate change mitigation on ocean acidification projections *Ocean Acidification* ed J-P Gattuso and L Hansson (Oxford: Oxford University Press) pp 273–89

[50] Steinacher M and Joos F 2016 Transient Earth system responses to cumulative carbon dioxide emissions: linearities, uncertainties, and probabilities in an observation-constrained model ensemble *Biogeosciences* **13** 1071–103

[51] Goodwin P, Brown S, Haigh I D, Nicholls R J and Matter J M 2018 Adjusting Mitigation Pathways to Stabilize Climate at 1.5°C and 2.0°C Rise in Global Temperatures to Year 2300 *Earth's Futur.* **6** 601–15

[52] Terhaar J, Frölicher T L, Aschwanden M T, Friedlingstein P and Joos F 2022 Adaptive emission reduction approach to reach any global warming target *Nat. Clim. Chang.* **12** 1136–42

[53] Lienert S and Joos F 2018 A Bayesian ensemble data assimilation to constrain model parameters and land-use carbon emissions *Biogeosciences* **15** 2909–30

[54] Roth R, Ritz S P and Joos F 2014 Burial-nutrient feedbacks amplify the sensitivity of atmospheric carbon dioxide to changes in organic matter remineralisation *Earth Syst. Dyn.* **5** 321–43

[55] Terhaar J, Frölicher T L and Joos F 2022 Observation-constrained estimates of the global ocean carbon sink from Earth System Models *Biogeosciences* **19** 4431–57

[56] Burger F A, Terhaar J and Frölicher T L 2022 Compound marine heatwaves and ocean acidity extremes *Nat. Commun.* **13** 4722

[57] Otto F E L, Frame D J, Otto A and Allen M R 2015 Embracing uncertainty in climate change policy *Nat. Clim. Chang.* **5** 917–20

[58] Joos F, Roth R, Fuglestvedt J S, Peters G P, Enting I G, von Bloh W, Brovkin V, Burke E J, Eby M, Edwards N R, Friedrich T, Frölicher T L, Halloran P R, Holden P B, Jones C, Kleinen T, Mackenzie F T, Matsumoto K, Meinshausen M, Plattner G-K, Reisinger A, Segschneider J, Shaffer G, Steinacher M, Strassmann K, Tanaka K, Timmermann A and Weaver A J 2013 Carbon dioxide and climate impulse response functions for the computation of greenhouse gas metrics: a multi-model analysis *Atmos. Chem. Phys.* **13** 2793–825

[59] Ritz S P, Stocker T F and Joos F 2011 A Coupled Dynamical Ocean–Energy Balance Atmosphere Model for Paleoclimate Studies *J. Clim.* **24** 349–75

[60] Battaglia G and Joos F 2018 Marine N2O Emissions From Nitrification and Denitrification Constrained by Modern Observations and Projected in Multimillennial Global Warming Simulations *Global Biogeochem. Cycles* **32** 92–121

[61] Arora V K, Katavouta A, Williams R G, Jones C D, Brovkin V, Friedlingstein P, Schwinger J, Bopp L, Boucher O, Cadule P, Chamberlain M A, Christian J R, Delire C, Fisher R A, Hajima T, Ilyina T, Joetzjer E, Kawamiya M, Koven C D, Krasting J P, Law R M, Lawrence D M, Lenton A, Lindsay K, Pongratz J, Raddatz T, Séférian R, Tachiiri K, Tjiputra J F, Wiltshire A, Wu T and Ziehn T 2020 Carbon–concentration and carbon–climate feedbacks in CMIP6 models and theircomparison to CMIP5 models *Biogeosciences* **17** 4173–222

[62] Sherwood S C, Webb M J, Annan J D, Armour K C, Forster P M, Hargreaves J C, Hegerl G, Klein S A, Marvel K D, Rohling E J, Watanabe M, Andrews T, Braconnot P, Bretherton C S, Foster G L, Hausfather Z, von der Heydt A S, Knutti R, Mauritsen T, Norris J R, Proistosescu C, Rugenstein M, Schmidt G A, Tokarska K B and Zelinka M D 2020 An Assessment of Earth's Climate Sensitivity Using Multiple Lines of Evidence *Rev. Geophys.* **58** e2019RG000678

[63] Battaglia G, Steinacher M and Joos F 2016 A~probabilistic assessment of calcium carbonate export \hack{\newline}and dissolution in the modern ocean *Biogeosciences* **13** 2823–48

[64] Friedlingstein P, Jones M W, O'Sullivan M, Andrew R M, Bakker D C E, Hauck J, Le Quéré C, Peters G P, Peters W, Pongratz J, Sitch S, Canadell J G, Ciais P, Jackson R B, Alin S R, Anthoni P, Bates N R, Becker M, Bellouin N, Bopp L, Chau T T T, Chevallier F, Chini L P, Cronin M, Currie K I, Decharme B, Djeutchouang L M, Dou X, Evans W, Feely R A, Feng L, Gasser T, Gilfillan D, Gkritzalis T, Grassi G, Gregor L, Gruber N, Gürses Ö, Harris I, Houghton R A, Hurtt G C, Iida Y, Ilyina T, Luijkx I T, Jain A, Jones S D, Kato E, Kennedy D, Klein Goldewijk K, Knauer J, Korsbakken J I, Körtzinger A, Landschützer P, Lauvset S K, Lefèvre N, Lienert S, Liu J, Marland G, McGuire P C, Melton J R, Munro D R, Nabel J E M S, Nakaoka S-I, Niwa Y, Ono T, Pierrot D, Poulter B, Rehder G, Resplandy L, Robertson E, Rödenbeck C, Rosan T M, Schwinger J, Schwingshackl C, Séférian R, Sutton A J, Sweeney C, Tanhua T, Tans P P, Tian H, Tilbrook B, Tubiello F, van der Werf G R, Vuichard N, Wada C, Wanninkhof R, Watson A J, Willis D, Wiltshire A J, Yuan W, Yue C, Yue X, Zaehle S and Zeng J 2022 Global Carbon Budget 2021 *Earth Syst. Sci. Data* **14** 1917–2005

[65] Ecofys, CA and PIK 2009 *Climate action tracker*

[66] Lamarque J-F, Bond T C, Eyring V, Granier C, Heil A, Klimont Z, Lee D, Liousse C, Mieville A, Owen B, Schultz M G, Shindell D, Smith S J, Stehfest E, Van Aardenne J, Cooper O R, Kainuma M, Mahowald N, McConnell J R, Naik V, Riahi K and van Vuuren D P 2010 Historical (1850–2000) gridded anthropogenic and biomass burning emissions of reactive gases and aerosols: methodology and application *Atmos. Chem. Phys.* **10** 7017–39

[67] Smith S J, Pitcher H and Wigley T M L 2001 Global and regional anthropogenic sulfur dioxide emissions *Glob. Planet. Change* **29** 99–119

[68] Bond T C, Bhardwaj E, Dong R, Jogani R, Jung S, Roden C, Streets D G and Trautmann N M 2007 Historical emissions of black and organic carbon aerosol from energy-related combustion, 1850–2000 *Global Biogeochem. Cycles* **21**

[69] Eyring V, Isaksen I S A, Berntsen T, Collins W J, Corbett J J, Endresen O, Grainger R G, Moldanova J, Schlager H and Stevenson D S 2010 Transport impacts on atmosphere and climate: Shipping *Atmos. Environ.* **44** 4735–71

[70] Lee D S, Fahey D W, Forster P M, Newton P J, Wit R C N, Lim L L, Owen B and Sausen R 2009 Aviation and global climate change in the 21st century *Atmos. Environ.* **43** 3520–37

[71] Forster P, Storelvmo T, Armour K, Collins W, Dufresne J L, Frame D, Lunt D J, Mauritsen T, Palmer M D, Watanabe M, Wild M and Zhang H 2021 The Earth's Energy Budget, Climate Feedbacks, and Climate Sensitivity ed V Masson-Delmotte, P Zhai, A Pirani, S L Connors, C Péan, S Berger, N Caud, Y Chen, L Goldfarb, M I Gomis, M Huang, K Leitzell, E Lonnoy, J B R Matthews, T K Maycock, T Waterfield, O Yelekçi, R Yu and B Zhou *Clim. Chang. 2021 Phys. Sci. Basis. Contrib. Work. Gr. I to Sixth Assess. Rep. Intergov. Panel Clim. Chang.*

[72] Hurtt G C, Chini L, Sahajpal R, Frolking S, Bodirsky B L, Calvin K, Doelman J C, Fisk J, Fujimori S, Klein Goldewijk K, Hasegawa T, Havlik P, Heinimann A, Humpenöder F, Jungclaus J, Kaplan J O, Kennedy J, Krisztin T, Lawrence D, Lawrence P, Ma L, Mertz O, Pongratz J, Popp A, Poulter B, Riahi K, Shevliakova E, Stehfest E, Thornton P, Tubiello F N, van Vuuren D P and Zhang X 2020 Harmonization of global land use change and management for the period850–2100 (LUH2) for CMIP6 *Geosci. Model Dev.* **13** 5425–64

[73] Gao C, Robock A and Ammann C 2008 Volcanic forcing of climate over the past 1500 years: An improved ice core-based index for climate models *J. Geophys. Res. Atmos.* **113**

[74] Schmidt G A, Jungclaus J H, Ammann C M, Bard E, Braconnot P, Crowley T J, Delaygue G, Joos F, Krivova N A, Muscheler R, Otto-Bliesner B L, Pongratz J, Shindell D T, Solanki S K, Steinhilber F and Vieira L E A 2012 Climate forcing reconstructions for use in PMIP simulations of the Last Millennium (v1.1) *Geosci. Model Dev.* **5** 185–91

[75] Fricko O, Havlik P, Rogelj J, Klimont Z, Gusti M, Johnson N, Kolp P, Strubegger M, Valin H, Amann M, Ermolieva T, Forsell N, Herrero M, Heyes C, Kindermann G, Krey V, McCollum D L, Obersteiner M, Pachauri S, Rao S, Schmid E, Schoepp W and Riahi K 2017 The marker quantification of the Shared Socioeconomic Pathway 2: A middle-of-the-road scenario for the 21st century *Glob. Environ. Chang.* **42** 251–67

[76] IPCC 2022 *Climate Change 2022: Mitigation of Climate Change. Contribution of Working Group III to the Sixth Assessment Report of the Intergovernmental Panel on Climate Change* ed P R Shukla, J Skea, R Slade, A Al Khourdajie, R van Diemen, D McCollum, M Pathak, S Some, P Vyas, R Fradera, M Belkacemi, A Hasija, G Lisboa, S Luz and J Malley (Cambridge, UK and New York, NY: Cambridge University Press)

[77] Robock A, Oman L and Stenchikov G L 2008 Regional climate responses to geoengineering with tropical and Arctic SO2 injections *J. Geophys. Res. Atmos.* **113**

[78] of Sciences Engineering and Medicine 2021 *Reflecting Sunlight: Recommendations for Solar Geoengineering Research and Research Governance* (Washington, DC: The National Academies Press)

[79] Dlugokencky E and Tans P Trends in Atmospheric Carbon Dioxide (NOAA/GML) *NOAA/GML*

[80] van Vuuren D P, Stehfest E, Gernaat D E H J, Doelman J C, van den Berg M, Harmsen M, de Boer H S, Bouwman L F, Daioglou V, Edelenbosch O Y, Girod B, Kram T, Lassaletta L, Lucas P L, van Meijl H, Müller C, van Ruijven B J, van der Sluis S and Tabeau A 2017 Energy, land-use and greenhouse gas emissions trajectories under a green growth paradigm *Glob. Environ. Chang.* **42** 237–50

[81] Morice C P, Kennedy J J, Rayner N A, Winn J P, Hogan E, Killick R E, Dunn R J H, Osborn T J, Jones P D and Simpson I R 2021 An Updated Assessment of Near-Surface Temperature Change From 1850: The HadCRUT5 Data Set *J. Geophys. Res. Atmos.* **126** e2019JD032361

[82] Torres O, Kwiatkowski L, Sutton A J, Dorey N and Orr J C 2021 Characterizing Mean and Extreme Diurnal Variability of Ocean CO2 System Variables Across Marine Environments *Geophys. Res. Lett.* **48** e2020GL090228

[83] Kwiatkowski L, Torres O, Aumont O and Orr J C 2022 Modified future diurnal variability of the global surface ocean CO2 system *Glob. Chang. Biol.* **n/a**

[84] Hauri C, Friedrich T and Timmermann A 2016 Abrupt onset and prolongation of aragonite undersaturation events in the Southern Ocean *Nat. Clim. Chang.* **6** 172–6

[85] Berge J, Renaud P E, Darnis G, Cottier F, Last K, Gabrielsen T M, Johnsen G, Seuthe L, Weslawski J M, Leu E, Moline M, Nahrgang J, Søreide J E, Varpe Ø, Lønne O J, Daase M and Falk-Petersen S 2015 In the dark: A review of ecosystem processes during the Arctic polar night *Prog. Oceanogr.* **139** 258–71

[86] Terhaar J, Tanhua T, Stöven T, Orr J C and Bopp L 2020 Evaluation of Data-Based Estimates of Anthropogenic Carbon in the Arctic Ocean *J. Geophys. Res. Ocean.* **125**

[87] Resplandy L, Bopp L, Orr J C and Dunne J P 2013 Role of mode and intermediate waters in future ocean acidification: Analysis of CMIP5 models *Geophys. Res. Lett.* **40** 3091–5

[88] Goris N, Tjiputra J F, Olsen A, Schwinger J, Lauvset S K and Jeansson E 2018 Constraining Projection-Based Estimates of the Future North Atlantic Carbon Uptake *J. Clim.* **31** 3959–78

[89] Bourgeois T, Goris N, Schwinger J and Tjiputra J F 2022 Stratification constrains future heat and carbon uptake in the Southern Ocean between 30°S and 55°S *Nat. Commun.* **13** 340

[90] Lauvset S K, Key R M, Olsen A, van Heuven S, Velo A, Lin X, Schirnick C, Kozyr A, Tanhua T, Hoppema M, Jutterström S, Steinfeldt R, Jeansson E, Ishii M, Perez F F, Suzuki T and Watelet S 2016 A new global interior ocean mapped climatology: the 11 GLODAP version 2 *Earth Syst. Sci. Data* **8** 325–40

[91] Meinshausen M, Lewis J, McGlade C, Gütschow J, Nicholls Z, Burdon R, Cozzi L and Hackmann B 2022 Realization of Paris Agreement pledges may limit warming just below 2 °C *Nature* **604** 304–9

[92] Hauri C, Pagès R, McDonnell A M P, Stuecker M F, Danielson S L, Hedstrom K, Irving B, Schultz C and Doney S C 2021 Modulation of ocean acidification by decadal climate variability in the Gulf of Alaska *Commun. Earth Environ.* **2** 191

[93] Gruber N, Hauri C, Lachkar Z, Loher D, Frölicher T L and Plattner G-K 2012 Rapid Progression of Ocean Acidification in the California Current System *Science (80-.).* **337** 220–3

[94] Franco A C, Gruber N, Frölicher T L and Kropuenske Artman L 2018 Contrasting Impact of Future CO2 Emission Scenarios on the Extent of CaCO3 Mineral Undersaturation in the Humboldt Current System *J. Geophys. Res. Ocean.* **123** 2018–36

[95] Griffies S M, Winton M, Anderson W G, Benson R, Delworth T L, Dufour C O, Dunne J P, Goddard P, Morrison A K, Rosati A, Wittenberg A T, Yin J and Zhang R 2015 Impacts on Ocean Heat from Transient Mesoscale Eddies in a Hierarchy of Climate Models *J. Clim.* **28** 952–77

[96] Dufour C O, Griffies S M, de Souza G F, Frenger I, Morrison A K, Palter J B, Sarmiento J L, Galbraith E D, Dunne J P, Anderson W G and Slater R D 2015 Role of Mesoscale Eddies in Cross-Frontal Transport of Heat and Biogeochemical Tracers in the Southern Ocean *J. Phys. Oceanogr.* **45** 3057–81

[97] Lachkar Z, Orr J C and Dutay J-C 2009 Seasonal and mesoscale variability of oceanic transport of anthropogenic CO$_{2}$ *Biogeosciences* **6** 2509–23

Supplementary Table 1. Overview of the 864 simulations with Bern3D-LPX. 3 simulation sets with 4 temperature targets, 9 Bern3D-LPX setups, and 8 different superimposed inter-annual variabilities.

Simulation sets (3)	‘baseline’			‘high-CO_2’			‘constant aerosol’		
CH_4 and N_2O emissions	according to SSP2-4.5			proportional to CO_2 emissions			proportional to CO_2 emissions		
Aerosol radiative forcing	exponential decay			exponential decay			constant		
Temperature Targets (4)	1.5°C			2.0°C			2.5°C		3.0°C
Bern3D-LPX setups (9)									
ECS [°C]	2.33	2.38	2.40	3.09	3.20	3.41	4.18	4.30	4.63
TCRE [°C]	1.35	1.38	1.45	1.66	1.69	1.77	2.03	2.08	2.16
ocean diapycnal mixing [$m^2\ s^{-1}$]	$3e^{-5}$	$2e^{-5}$	$1e^{-5}$	$3e^{-5}$	$2e^{-5}$	$1e^{-5}$	$3e^{-5}$	$2e^{-5}$	$1e^{-5}$
climate feedback parameter [$W\ m^{-2}\ K^{-1}$]	-1.0	-1.0	-1.0	-0.5	-0.5	-0.5	-0.1	-0.1	-0.1
Inter-annual variabilities (8)	100-year inter-annual variability is added and subtracted with four different phasing								

Supplementary Table 2. Projected carbon cycle and ocean acidification under various temperature targets. Remaining CO_2 emissions from 2021 to 2150 that allow meeting the temperature targets, atmospheric CO_2 in 2150, cumulative ocean carbon uptake from 1765 to 2150, globally averaged surface ocean pH in 2150, and the additionally undersaturated waters towards aragonite from 2002 to 2150.

Global warming levels	1.5°C		2.0°C		2.5°C		3.0°C	
	baseline	high-CO_2	baseline	high-CO_2	baseline	high-CO_2	baseline	high-CO_2
Remaining CO_2 emissions from 2021 to 2150 (Pg C)	-236 - 25	54 - 286	-25 - 404	239 - 584	187 - 798	426 - 865	401 – 1083	611 - 1047
Atmospheric CO_2 in 2150 (ppm)	320 - 368	371 - 420	356 - 448	408 - 490	399 - 547	453 - 569	451 - 639	508 - 636
Cumulative ocean carbon uptake from 1765 to 2150 (Pg C)	190 - 271	281 - 352	259 - 396	336 - 446	329 - 504	390 - 519	391 - 568	435 - 560
Globally averaged surface ocean pH in 2150	8.08 – 8.13	8.03 – 8.08	8.01 – 8.09	7.98 - 8.05	7.94 – 8.05	7.92 – 8.01	7.88 – 8.01	7.88 – 7.97
Volume of additional undersaturated waters towards aragonite from 2002 to 2150 (10^6 km^3)	47 - 86	86 - 111	81 - 124	109 - 137	108 - 154	127 - 158	129 - 170	142 - 168

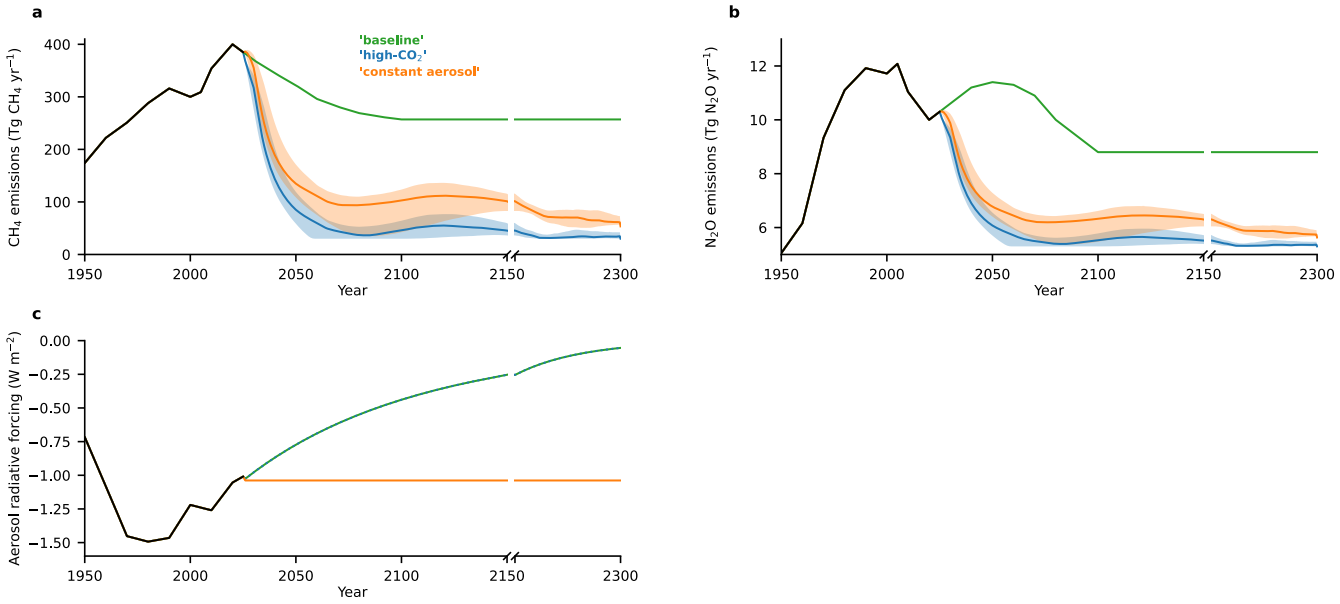

631

632 **Supplementary Figure 1. CH_4 and N_2O emissions and aerosol radiative forcing for the three scenarios. a)** Global CH_4 and **b)** N_2O

633 emissions, as well as **c)** aerosol radiative forcing over the historical period until 2025 (black line) and from 2025 to 2300 under the 'baseline'

634 scenario (green), 'high-CO_2' scenario (blue), and 'constant aerosol' scenario (orange). The colored lines indicate simulations with the model

635 setup that has an ECS of 3.2°C, the central estimate according to Sherwood et al. (2020) [62]. The shading indicates the range of all model

636 setups with ECS' from 2.3 to 4.7°C (5-95% ECS likelihood range) [62].

637

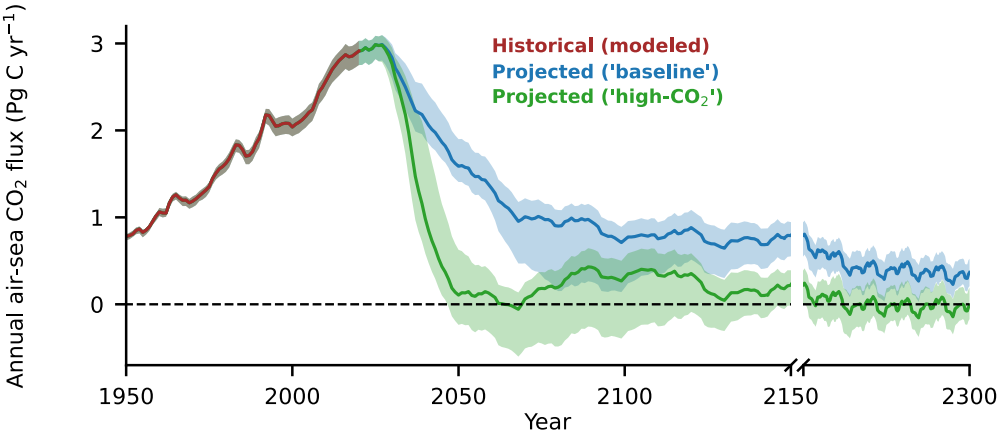

638

639 **Supplementary Figure 2. Annual air-sea CO2 fluxes for the 1.5°C target under the '*baseline*' and '*high-CO_2*' scenarios.** Global annual
640 mean air-sea CO_2 fluxes since 1950 as simulated by the Bern3D-LPX. Historical fluxes until 2020 (brown) and projections after 2020 are
641 shown for the 1.5°C target for the 'baseline' (green) and 'high-CO_2' (blue) scenarios. The dashed black lines show zero fluxes. The green
642 and blue lines indicate simulations with the model setup that has an ECS of 3.2°C, the central estimate according to Sherwood et al. (2020)
643 [62]. The shading indicates the range of all model setups with ECS' from 2.3 to 4.7°C (5-95% ECS likelihood range) [62].

644

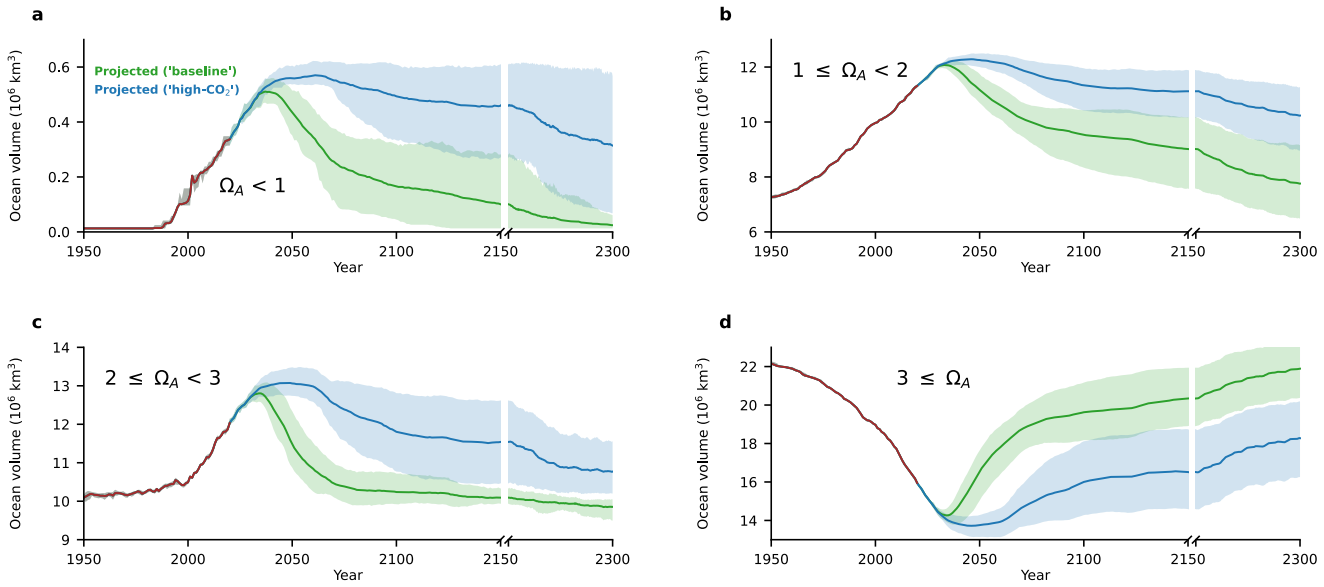

Supplementary Figure 3. Ocean aragonite saturation state over time in the upper 126 m of the ocean. Global mean ocean volume between the surface and 126 m depth of water masses with aragonite saturation states **a)** below 1, **b)** between 1 and 2, **c)** between 2 and 3, and **d)** above 3 as simulated by the Bern3D-LPX until 2020 (brown) and from 2020 to 2300 for the 1.5°C target under the 'baseline' (green) and 'high-CO_2' (blue) scenario. The lines indicate simulations with the model setup that has an ECS of 3.2, the central estimate according to Sherwood et al. (2020) [62]. The shading indicates the range of all model setups with ECSs from 2.3 to 4.7°C (5-95% ECS likelihood range [62]. Saturation states in 2002 are calculated from observation-based global ocean estimates of dissolved inorganic carbon, alkalinity, temperature, salinity, silicon, and phosphorus from GLODAPv2 [90]. For all other years, saturation states are calculated from the observation-based dissolved inorganic carbon, alkalinity, temperature, salinity, silicon, and phosphorus in 2002 plus the respective simulated changes in with respect to 2002 [23,37,40].

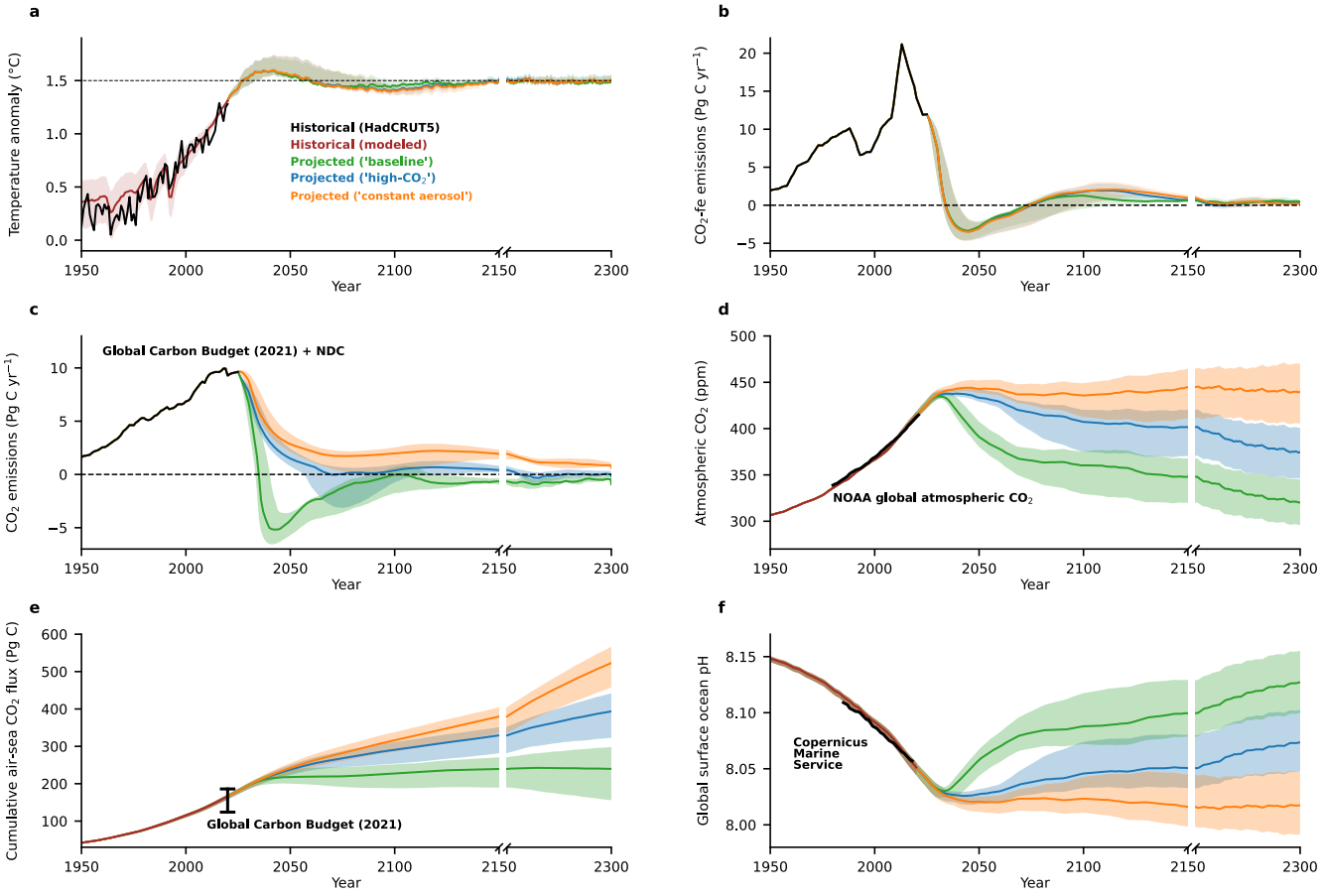

Supplementary Figure 4. Temperature anomalies, associated CO_2 forcing equivalent emissions, and carbon cycle dynamics for the 'constant aerosol' scenario. a) Global mean surface temperature anomalies over the historical period until 2020 as observed by HadCRUT5 [81] (black line) and as simulated by the Bern3D-LPX (brown). After 2020, projections are shown for the 1.5°C target for the 'baseline' (green), 'high-CO_2' (blue), and 'constant aerosol' (orange) scenarios. The dashed black lines show the 1.5°C temperature target. **b)** CO_2 forcing equivalent (CO_2-fe) emissions and **c)** CO_2 emissions as prescribed from the Global Carbon Budget 2021 [64] and NDCs until 2025 (black) and adaptively developed by the AERA from 2025 onwards. The dashed line represents zero emissions. Simulated **d)** atmospheric CO_2, **e)** cumulative air-sea CO_2 flux since 1765, and **f)** globally averaged surface ocean pH. The green and blue lines indicate simulations with the model setup that has an ECS of 3.2°C, the central estimate according to Sherwood et al. (2020) [62]. The shading indicates the range of all model setups with ECS' from 2.3 to 4.7°C (5-95% ECS likelihood range) [62]. In addition, observation-based estimates of the **d)** past global atmospheric CO_2 from NOAA averaged over marine surface sites [79], the **e)** historical cumulative ocean carbon uptake from the Global Carbon Budget 2021 [64], and the **f)** past global surface average pH from the Copernicus Marine Service (https://doi.org/10.48670/moi-00047) is shown.